

Dual Single Pixel Imaging in SWIR using Compressed Sensing

Martin Oja¹, Sebastian Olsson¹, Carl Brännlund²^a, Andreas Brorsson²^b, David Bergström²^c and David Gustafsson²^d

¹Linköping University, Linköping, Sweden

²FOI - Swedish Defence Research Agency, CAISR, Linköping, Sweden

Keywords: Compressive Sensing, Single Pixel Imaging, Complementary Sampling, SWIR, Total Variation.


Abstract: In this paper, we present a dual Single Pixel Camera (SPC) operating in the Short Wave InfraRed (SWIR) spectral range that reconstructs high resolution images from an ensemble of compressed measurements. The SWIR spectrum provides significant benefits in many applications due to its night vision capabilities and its ability to penetrate smoke and fog. Walsh-Hadamard matrices are used for generating pseudo-random measurements which speed up the reconstruction and enable reconstruction of high resolution images. Total variation regularization is used for finding a sparse solution in the gradient space. The detectors have been fitted with analog filters and amplification in order to capture scenes in low light. A number of outdoor scenes with varying illumination have been collected using the dual single pixel sensor. Visual inspection of the reconstructed SWIR images indicate that most scenes and objects can be identified with a lower subsampling ratio (SR) compared to a single detector setup. The image quality is consistently better than with one detector, with similar results achieved with fewer samples or better results with the same number of samples. We also present measurements on moving objects in the scene and movements in the SPC unit and compare the results between single and dual detectors.


1 INTRODUCTION


Conventional focal plane array cameras capture the scene by measuring the light incident at each of the thousands of pixels instantly. In Compressed or Compressive Sensing (CS) a relatively small number of measurements with a Single Pixel Camera (SPC) using a single detector and a Spatial Light Modulator (SLM), which changes pattern for each measurement, are combined with a sparse reconstruction procedure to recover a high resolution image. CS or when dealing with images, Compressive Imaging (CI) exploits the fact that natural images are compressible or sparse in some basis and therefore only a few measurements relative to the image resolution are needed to reconstruct the image. M measurements are sampled to reconstruct an image with N pixels, where $M \ll N$, far fewer samples than required by the NyquistShannon sampling theorem. Two constraints must be fulfilled in order to utilize CS sampling: the image needs to


be compressible and the measurement matrix needs to be incoherent with the sparse transform. The first constraint is fulfilled because natural images are compressible using for example JPEG or JPEG2000 (using wavelet transform) and the second constraint is fulfilled using a measurement matrix with a random characteristic. Although the light from the scene is modulated by far fewer patterns on the SLM than the image resolution, capturing a high quality image with a SPC can be a time-consuming task. When reconstructing an image, the CS-algorithms assumes the scene to be stationary, so a SPC is sensitive to any type of scene variations. Decreasing this sensitivity as well as increasing the image quality and frame rate are important goals for the development of SPCs.

The interest in SPCs is motivated by applications where sensors are very costly, such as imaging in the Short-Wave Infrared (SWIR) spectrum. In many applications the SWIR spectrum provides significant benefits over the visual spectrum. For example SWIR enables separation between camouflage and vegetation, and penetrates to some extent fog and smoke which enables imaging through scattering media. Furthermore, SWIR sensors can be used for

^a  <https://orcid.org/0000-0002-4047-2083>

^b  <https://orcid.org/0000-0002-3922-9334>

^c  <https://orcid.org/0000-0003-2414-4482>

^d  <https://orcid.org/0000-0002-4370-2286>

passive imaging in the dark due to the night-glow of the sky.

The twin, double or dual SPC (DSPC) presented in this paper combines a Digital Micromirror Device (DMD), two nearly identical InGaAs photodiodes, an analog amplifier with a band-pass filter and an Analog to Digital Converter (ADC). The second detector measures the complementary patterns which are the "dark" mirrors of the patterns not visible from the first detector. Because the two detectors measure all the light reflected off the DMD, they can produce higher quality images, or the same quality at a lower SR, thus increasing the frame rate. Using an extra detector also reduces sensitivity to scene and light variations, weather, turbulence and movement in the SPC unit. The amplifier unit improves low light performance and the band-pass filter blocks the DC-level and high frequency noise. The two outputs are sampled by the ADC and can in the software be combined to a single signal, to be restored to one high quality image or two lower quality images (one for each detector). In this paper the main goal is to investigate the difference between using one and two detectors. The system is evaluated and the increase in image quality and Signal-to-Noise Ratio (SNR) is measured with one and two detectors. Results from static and moving outdoor natural scenes with different lighting condition and SR are presented, as well as a measurement with small movements in the SPC-system (the system is shaken by hand).

In 2014 (Yu et al., 2014) presented a similar setup with two photomultiplier tubes and investigated the potential for increase in performance for the first time. A system with two detectors using a balanced amplifier was presented for the first time in 2016 (Soldevila et al., 2016). This increases the frame rate and SNR, as well as improving performance in the presence of ambient light. The balanced detection also reduces electrical and quantization errors. Other examples of systems with two detectors have been described in papers such as (Czajkowski et al., 2018), which uses measurement matrices based on Morlet wavelets convolved with white noise to reduce the signal acquisition time, and (Lochocki et al., 2016), which evaluates the performance and demonstrates increased frame rate. A system with two different spectral band detectors (visual + SWIR) has also been demonstrated by (Welsh, 2017). A SPC with multiple detectors (RGB and SWIR) in the same DMD reflection direction was presented by (Edgar et al., 2015). SPCs in the SWIR band have been presented earlier and an example of a high resolution SPC with one detector is presented by (McMackin et al., 2012). The same measurements and DSPC design used in this paper

are also described in a thesis (Oja and Olsson, 2019). A paper by (Brännlund and Gustafsson, 2017), shows the initial results and proof of concept of the SWIR SPC architecture with one detector. The same design is improved in a thesis by Brorsson (Brorsson, 2018), which is also described in the paper (Brorsson et al., 2019).

2 COMPRESSIVE SENSING

2.1 Sparse Reconstruction

CS is a sampling strategy for acquiring and reconstructing a sparse signal, such as an image, by finding solutions to underdetermined linear systems where the number of measurements can be far fewer than required by the Nyquist-Shannon sampling theorem. Two constraints need to be fulfilled to apply CS sampling: the sampled image needs to be sparse in some basis, and the measurement matrix must be incoherent with the sparse transform. In CS the sampling model is defined as

$$\mathbf{y} = \Phi \mathbf{x} + \varepsilon, \quad (1)$$

where $\mathbf{x}_{N \times 1}$ is the scene considered as an image rearranged as an array with N pixels, $\mathbf{y}_{M \times 1}$ is the sampled signal with M measurements, $\Phi_{M \times N}$ is the measurements matrix and ε is the noise. The subsampling ratio is defined as $SR = M/N$, and this number can be relatively small compared to how compressible the image is. This is because the image \mathbf{x} can be represented as

$$\Psi \theta = \mathbf{x}, \quad (2)$$

where $\Psi_{N \times N}$ is some basis matrix and $\theta_{N \times 1}$ is the coefficients where θ is K -sparse. K -sparse means that the image \mathbf{x} has K non-zero elements in basis Ψ , $\|\theta\|_0 = K$. Given (2), (1) can be expanded to

$$\mathbf{y} = \Phi \mathbf{x} + \varepsilon = \Phi \Psi \theta + \varepsilon = \mathbf{A} \theta + \varepsilon, \quad (3)$$

where, $\mathbf{A}_{M \times N} = \Phi \Psi$ is called the reconstruction matrix. The revelation in (3) is what makes CS powerful. By sampling the scene using the measurement matrix Φ (as in (1)), but then in the reconstruction process transforming the measurement matrix Φ to the reconstruction matrix \mathbf{A} using some basis Ψ , the optimization algorithm can solve the system for the sparse coefficients θ instead of the dense spatial image coefficients in \mathbf{x} (Rish and Grabarnik, 2014).

2.2 Total Variation Regularization

The total variation (TV) based TVAL3 (Total Variation Augmented Lagrangian Alternating Direction Algorithm) is used for image reconstruction. Natural images often contain sharp edges and piecewise smooth areas which the TV regularization algorithm is good at preserving. The main difference between TV and other reconstruction algorithms is that TV considers the gradient of signal to be sparse instead of the signal itself, thus finding the sparsest gradient. The TV optimization problem in TVAL3 is defined as

$$\min_{\mathbf{x}} \sum_i \|D_i \mathbf{x}\|, \text{ subject to } \Phi \mathbf{x} = y, \mathbf{x} \geq 0, \quad (4)$$

where $D_i \mathbf{x}$ is the discrete gradient of \mathbf{x} at position i . TVAL3 is an optimization method for solving constrained problems by substituting the original constrained problem with a series of unconstrained sub-problems and introducing a penalty term. To solve the new sub-problems the alternating direction method is used (Li, 2010).

2.3 Permuted Sequence Ordered Walsh-Hadamard Matrix

In addition to eliminating the need to store the large measurement matrix in computer memory for reconstruction, the Permuted Sequence Ordered Walsh-Hadamard matrix (PSOWHM) can be generated when sent to the DMD and thus eliminating the need to store the matrix. PSOWHM has approximately the same characteristics and properties as an independent and identically distributed (i.i.d.) random matrix but generally has a higher number of measurements for exact reconstruction of the image. Research has however shown that there is no significant loss in recovery of the image relative to the i.i.d. random matrices (Zhuoran et al., 2013).

3 DUAL SINGLE PIXEL CAMERA ARCHITECTURE

The DSPC platform consists of a DMD (DLP4500NIR, 912×1140 , 700 – 2500 nm), two identical large area InGaAs-detectors with built-in amplifiers (PDA20C/M, 800 – 1700 nm) and an aluminium Newtonian telescope, which consists of a concave primary mirror (108 mm, F4.1), and a flat secondary mirror. This design has a maximum field of view of $22 \times 14 \mu rad$, which gives highly detailed scenes from a great distance. The motivation to use

a reflective optical system is partly that chromatic aberration is eliminated and partly that it works over a wide wavelength band. A visual spectrum reference camera is mounted viewing the DMD via a mirror in front of one of the detectors to simplify setup and focusing of the system. This mirror is removed when capturing images with the SPC. The lenses in front of the detectors have a diameter of 50.8 mm and a focal length of 32 mm (ACL50832U).

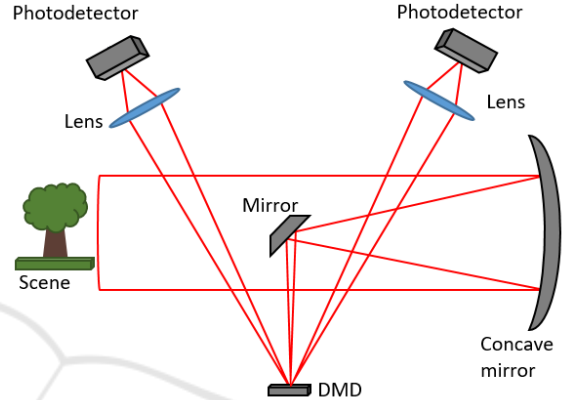


Figure 1: Illustration of the designed Dual Single Pixel Camera (DSPC).

The pseudo-random patterns are generated in C++ when streamed via HDMI as 24-bit images from a Windows computer to the control unit (DLP LightCrafter™ 4500). This unit is setup to split the received 24-bit image into 1-bit planes which are displayed in consecutive order. The control unit can be operated at a maximum speed of 2880 Hz (24-bit@120 Hz), but for synchronization reasons with the 60 Hz computer display only 1440 Hz was achieved (24-bit@60 Hz). At this rate a 512×512 measurement with a subsampling ratio of 10% is streamed in 17 seconds. Walsh-Hadamard matrices up to 512×512 (PSOWHM) are used for generating pseudo-random patterns. An open source total variation regularization algorithm (TVAL3) is used for finding a sparse solution in the gradient space.

The amplifier unit is designed with a band pass filter (100-13000 Hz) to remove the DC level as well as high and low frequency noise, coming from, for example, the electrical grid. The prototype was designed using potentiometers to be able to easily change the cut off frequency and gain. The two outputs from the amplifier are then greatly oversampled with an ADC (PicoScope 2406B).

3.1 Signal Processing

In our experiments the two detector signals are combined using the formula

$$y = y_A - y_B \quad (5)$$

where y_A and y_B are the signals from the two identical detectors. The reconstructed image using the combined signal y will result in an image with a higher quality, as well as reduced sensitivity to dynamic scene variations, than y_A or y_B on their own. It is noteworthy that this formula cancels out global light changes during the measurements, and that the sum of the two detector signals is constant, independent of the pattern on the DMD, $y_A + y_B \approx \text{const.}$ The mean value of y_A and y_B is zero because we filter out the DC-part of the signal, which also leads to $y_A + y_B \approx 0$.

Since the amplitude of the signals from the detectors varies depending on the light intensity, the gain needs to be set to match the ADC reference voltage. In bright sunlight there is little need for amplification since the amplitude is high enough to be measured with good resolution by the ADC, whereas in darker conditions a higher gain is needed. An example of a low light level signal from one detector with and without amplification sampled by the ADC, can be seen in Figure 2. An example of the signals from the two detectors sampled by the ADC can be seen in Figure 3.

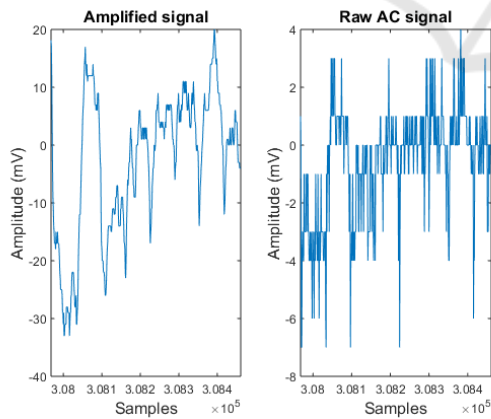


Figure 2: An example of an amplified (left) and unamplified (right) signal sampled by the ADC. Because of the band-pass (100-13000 Hz) filter the signals are centered at zero. The reference voltage is set to ± 250 mV.

The two output signals from the amplifier unit are greatly oversampled by the ADC, such that a single value corresponding to each pattern on the DMD could be obtained, as seen in Figure 4. This is performed in two steps; first we omit samples when the

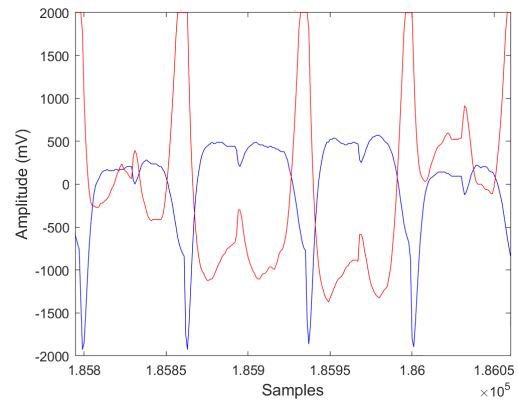


Figure 3: An example of the signals from the two detectors sampled by the ADC. Because of the band-pass (100-13000 Hz) filter the signals are centered at zero. Large positive and negative spikes occur when the patterns is changed on the DMD. A smaller spike is also visible in the middle of the pattern.

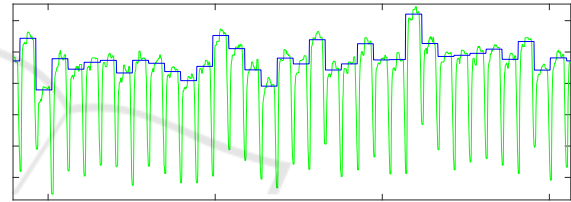


Figure 4: Signal measured using one detector (green) and the mean values (blue) for each DMD pattern. The mean values are calculated by omitting samples near the pattern transition (seen as negative spikes).

DMD is changing pattern (a short negative or positive spike in the signal dependent on which detector is measured), then the mean is calculated for each pattern. An array with one value per pattern $\mathbf{y}[m]$, is finally created.

4 EXPERIMENTS

To compare the performance of a SPC with one and two identical detectors multiple tests were conducted on both stationary and moving targets, as well as when small movements on the SPC system were induced by hand. In all the presented experiments the light level was quite high so the amplifier made little difference to the image quality. The number of active micromirrors in the measurements was always 512×512 (the mirrors are binned together at lower resolutions) independent of image resolution, which means that the field of view is always the same. Images of the same data were for a double detector system restored using $y = y_A - y_B$, or when considered as a single detector system $y = y_A$ as input

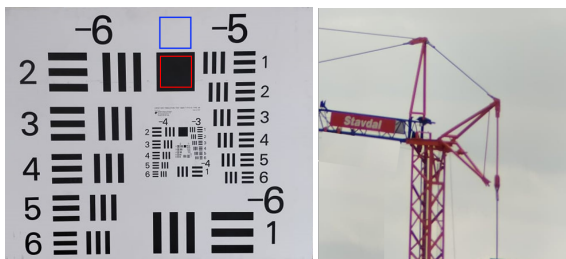


Figure 5: Left: The resolution board used in the experiments, the blue and red boxes represent the white and black uniform areas used for SNR calculations. Right: The construction crane used in some of the experiments.

to TVAL3. Restored images using y_A or y_B produced almost identical results in the experiments.

In order to measure the image quality, a series of tests at varying resolutions were conducted on a resolution board, outdoors at a distance of 90 m. The SNR for an image was then determined with

$$SNR = 2 \frac{\mu_1 - \mu_2}{(\sigma_1 + \sigma_2)} \quad (6)$$

where the mean value μ_1 and standard deviation, σ_1 corresponds to a white area, and μ_2 and σ_2 corresponds to a black area. The resolution board can be seen in Figure 5 where the white and black areas are marked. The difference between the two areas can be considered to be the signal strength.

5 RESULTS

In this section a selection of reconstructed images and SNR data, from stationary scenes, as well as dynamic measurements are presented. The reconstructed images of a stationary resolution board, placed outdoors at a relatively short range (90 m), can be seen in Figures 6, 7 and 8 at the resolutions 128×128 , 256×256 and 512×512 . The SNR for the same scene is presented in Figures 9, 10 and 11, where these graphs does not directly correlate to the presented images, because the images are reconstructed from one single measurement while the SNR has been calculated as mean values from multiple measurements. In Figure 12 images at 256×256 , with varying SR of a stationary construction crane at a distance of around 1000 m, can be seen. As can be seen the image quality is clearly higher for all SR. Figure 13 shows images at 512×512 with 1% SR, of the same crane when stationary and rotating. The crane was stationary in the beginning and end of the measurement, which can be seen in Figures a, d, e and h. In the middle of the measurement the crane was rotating which can be seen in

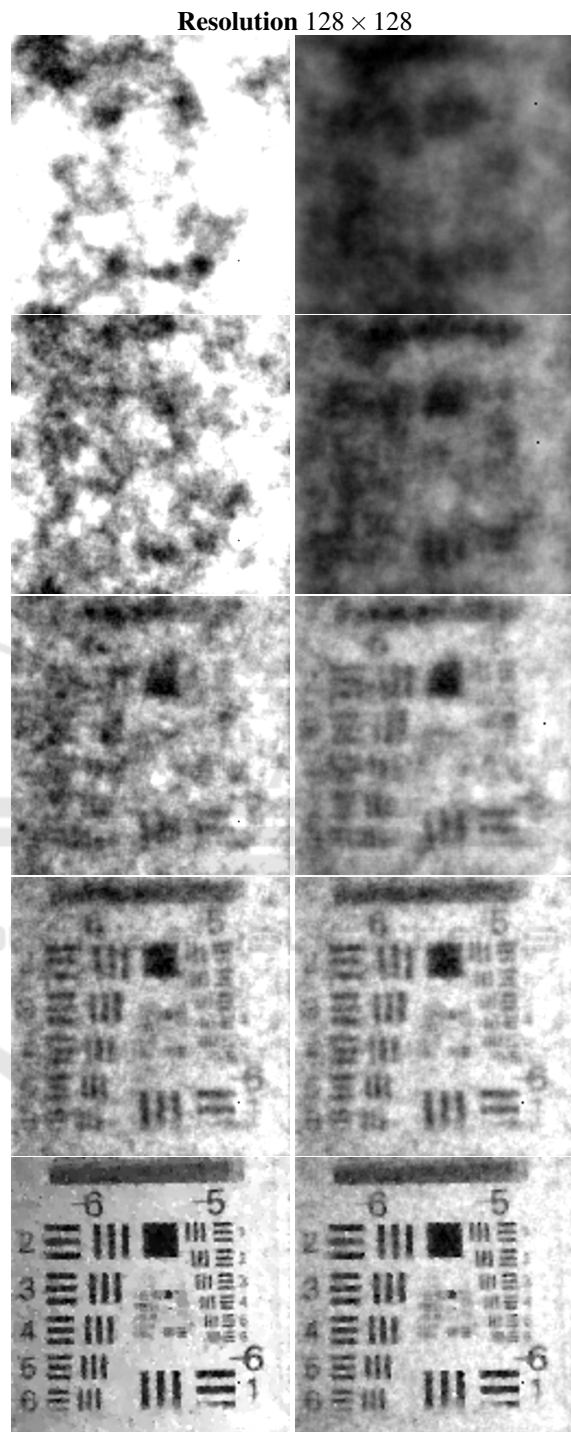


Figure 6: Reconstructed images at 128×128 of a resolution board at 90 m. Images are reconstructed using signals from one (left) and two (right) detectors. The SR from top to bottom is 1%, 3%, 7%, 17% and 35%. As can be seen the largest image quality difference is at low SR.

Figures b, c, f and g. Results of another measurement are presented in Figure 14, where small movements

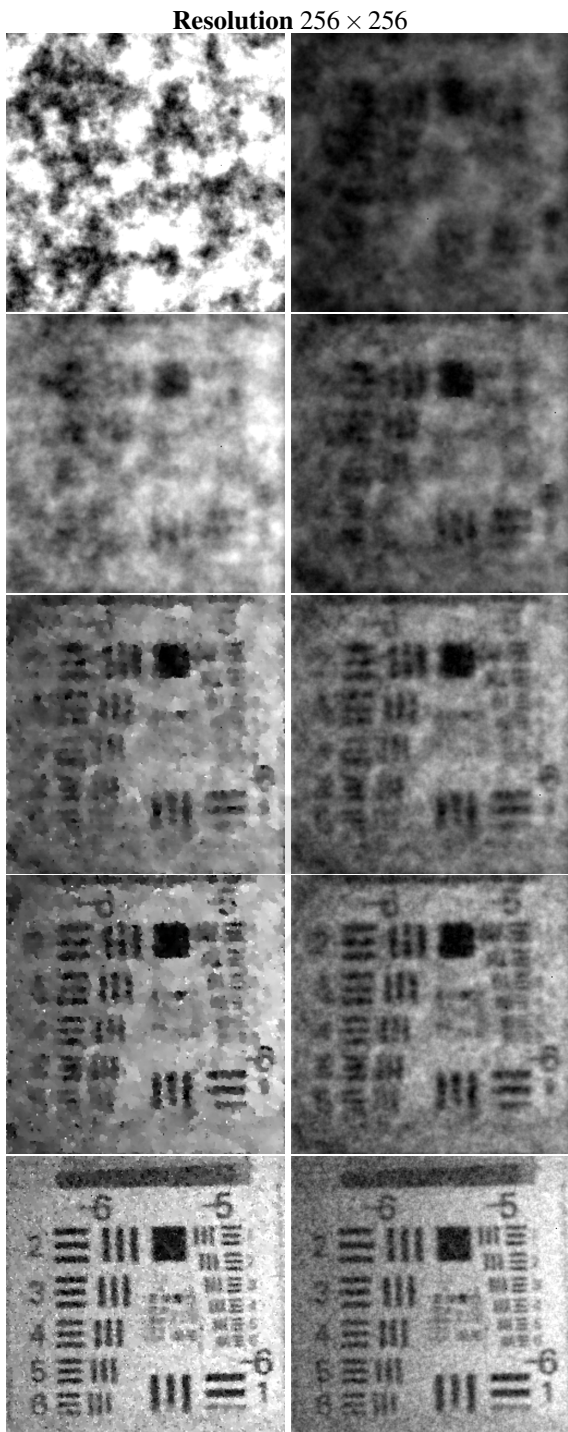


Figure 7: Reconstructed images at 256×256 of a resolution board at 90 m. Images are reconstructed using signals from one (left) and two (right) detectors. The SR from top to bottom is 1%, 2%, 4%, 7% and 30%. As can be seen the largest image quality difference is at low SR.

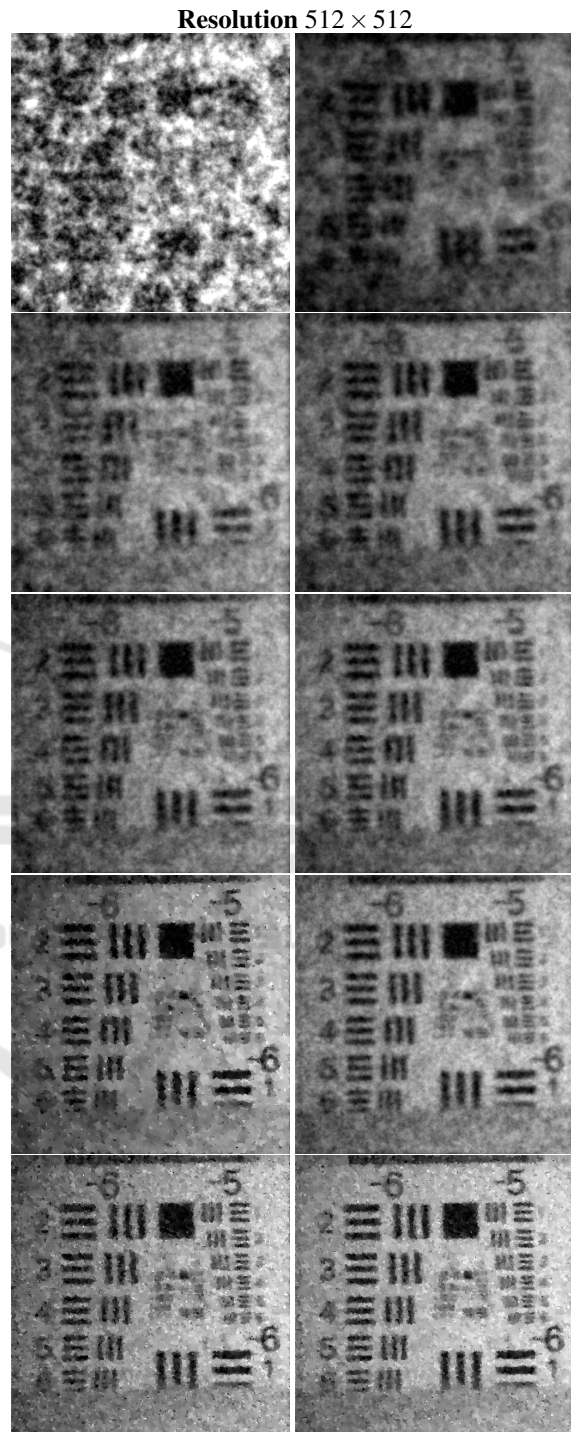


Figure 8: Reconstructed images at 512×512 of a resolution board at 90 m. Images are reconstructed using signals from one (left) and two (right) detectors. The SR from top to bottom is 1%, 2%, 3% and 10%. As can be seen the largest image quality difference is at low SR.

in the SPC system during the measurement were induced by hand.

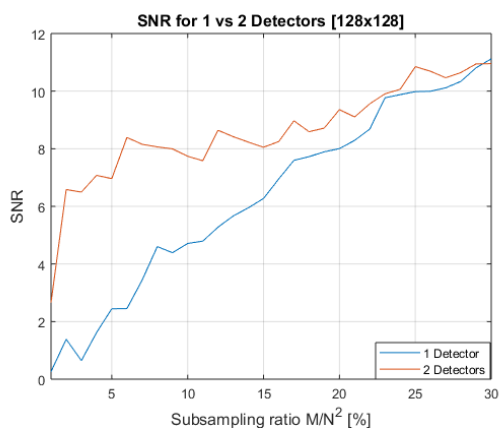


Figure 9: SNR for a resolution of 128×128 . Multiple measurements are performed and the SNR is calculated as a mean value.

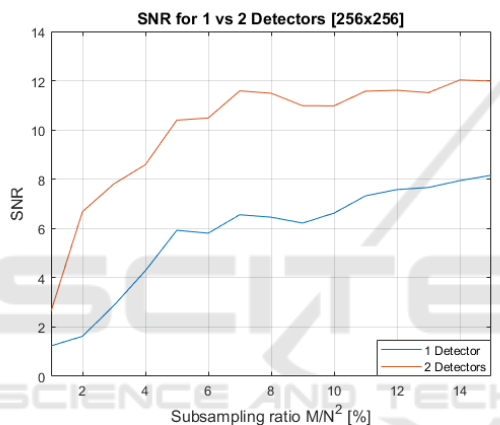


Figure 10: SNR for a resolution of 256×256 . Multiple measurements are performed and the SNR is calculated as a mean value.

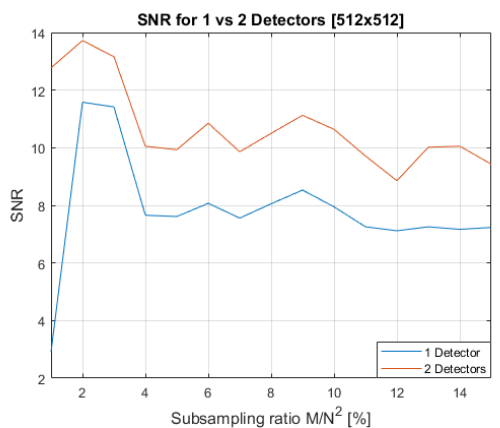


Figure 11: SNR for a resolution of 512×512 . Multiple measurements are performed and the SNR is calculated as a mean value.

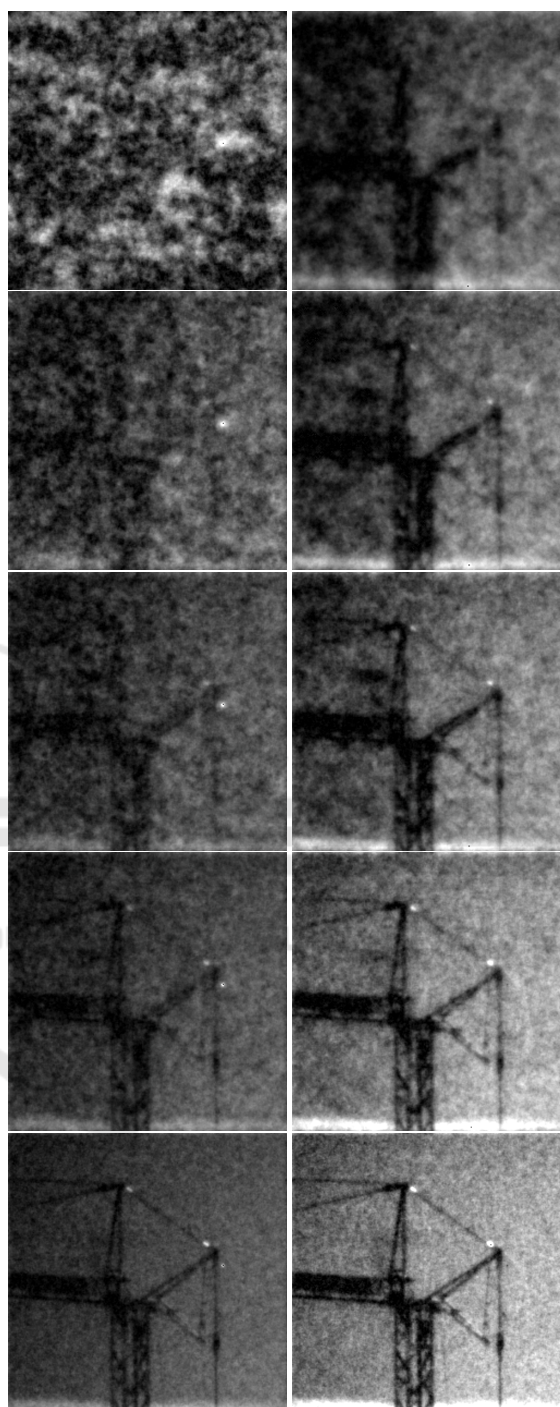
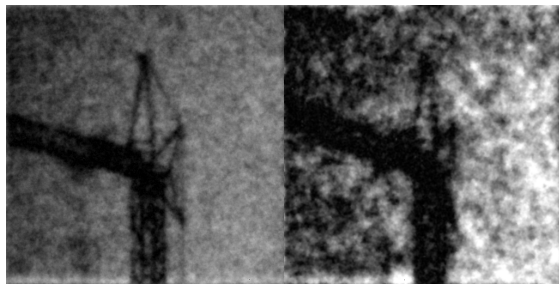
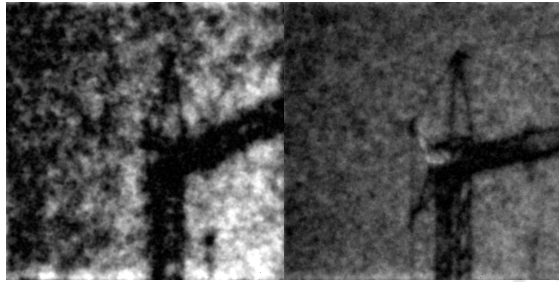


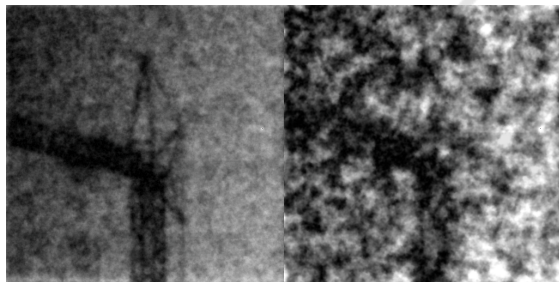
Figure 12: Reconstructed images at 256×256 of a stationary construction crane at different SR using one (left) and two detectors (right). The SR from top to bottom is 2%, 4%, 6%, 10% and 20%. As can be seen the largest quality difference is at low SR. It is also noteworthy that the image is brighter using two detectors.



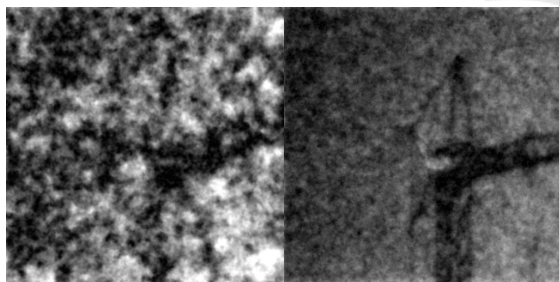
(a) Start, 2 detectors (b) Movement, 2 detectors



(c) Movement, 2 detectors (d) End, 2 detectors



(e) Start, 1 detector (f) Movement, 1 detector



(g) Movement, 1 detector (h) End, 1 detector

Figure 13: Reconstructed images at 512×512 and $SR = 1\%$ of a stationary and rotating construction crane. The subfigures (a) to (d) are captured with two detectors and (e) to (f) with one detector. Start is just before the movement started and End is after the movement stopped. The image quality of the moving crane is improved significantly with two detectors.

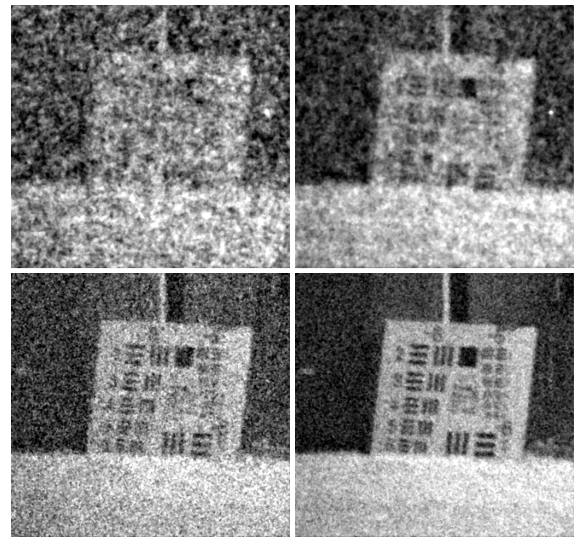


Figure 14: Reconstructed images at 512×512 of the resolution board placed against a wall at 126 m, with one (left) and two detectors (right). Vibrations/movements are induced by hand in the SPC system during the measurement. The SR from top to bottom is 5% and 20%. As can be seen the quality is significantly higher using two detectors for all SR.

6 CONCLUSIONS

What we consistently can see from the experiments is that an extra detector will always produce higher quality images with less noise, especially at low SR, where the image quality is significantly improved. By adding a second detector, the frame rate can be significantly improved if a low quality, usable image is acceptable. Our tests also show that a second detector makes a significant difference when capturing scenes with dynamics (light variations, movements in scene, movements of the SPC, etc.). Figure 13 is an example of this, when the moving crane is reconstructed using only 1% SR, and the differences between one and two detectors are very clear. The improvement in image quality is also clear in Figure 14 where small movements were induced in the SPC system. What should also be noted is that the calculated SNR is not an exact measure of image quality, where other factors such as edge response and sharpness are also important. This is obvious when comparing Figures 8 and 11 where the quality of the images is improved with increasing SR, while the measured SNR decreases when SR increases. The addition of an analog band-pass filter and especially the amplification enabled the SPC to produce images in poor weather conditions where the signal is weak. However, in good weather with a strong raw signal the filtering and amplification did little to improve the signal other than ensuring the sig-

nal is close to the reference voltage of the ADC.

REFERENCES

- Brännlund, C. and Gustafsson, D. (2017). Single pixel swir imaging using compressed sensing. In *Swedish Symposium on Image Analysis (SSBA)*. Swedish Symposium on Image Analysis (SSBA).
- Brorsson, A. (2018). Compressive sensing: Single pixel swir imaging of natural scenes. Master's thesis, Linköpings Universitet (LiTH-ISY-EX-18/5108-SE).
- Brorsson, A., Brännlund, C., Bergström, D., and Gustafsson, D. (2019). Compressed imaging at long range in swir. In *Scandinavia Conference on Image Analysis (SCIA)*. Springer International Publishing.
- Czajkowski, K. M., Pastuszczyk, A., and Kotyński, R. (2018). Single-pixel imaging with morlet wavelet correlated random patterns. *Scientific Reports*, 8(466).
- Edgar, M. P., Gibson, G. M., Bowman, R. W., Sun, B., Radwell, N., Mitchell, K. J., Welsh, S. S., and Padgett, M. J. (2015). Simultaneous real-time visible and infrared video with single-pixel detectors. *Scientific Reports*, 5.
- Li, C. (2010). An efficient algorithm for total variation regularization with applications to the single pixel camera and compressive sensing. Master's thesis, Rice University.
- Lochocki, B., Gambín-Regadera, A., and Artal, P. (2016). Performance evaluation of a two detector camera for real-time video. *Applied optics*, 55(36):10198–10203.
- McMackin, L., Herman, M. A., Chatterjee, B., and Weldon, M. (2012). A high-resolution swir camera via compressed sensing. In *Infrared Technology and Applications XXXVIII*, volume 8353, pages 48 – 57. International Society for Optics and Photonics, SPIE.
- Oja, M. and Olsson, S. (2019). Stand-alone dual sensing single pixel camera in swir. Master's thesis, Linköpings Universitet (LiU-ITN-TEK-A-19/024-SE).
- Rish, I. and Grabarnik, G. (2014). *Sparse Modeling: Theory, Algorithms, and Applications*. Chapman & Hall/CRC Machine Learning & Pattern Recognition. CRC Press, 1st edition.
- Soldevila, F., Clemente, P., Tajahuerce, E., Uribe-Patarroyo, N., Andrs, P., and Lancis, J. (2016). Computational imaging with a balanced detector. *Scientific Reports*, 6.
- Welsh, S. S. (2017). *Applications of single-pixel imaging*. PhD thesis, University of Glasgow.
- Yu, W.-K., Liu, X.-F., Yao, X.-R., Wang, C., Zhai, Y., and Zhai, G.-J. (2014). Complementary compressive imaging for the telescopic system. *Scientific Reports*, 4(5834).
- Zhuoran, C., Honglin, Z., Min, J., Gang, W., and Jingshi, S. (2013). An improved hadamard measurement matrix based on walsh code for compressive sensing. In *2013 9th International Conference on Information, Communications & Signal Processing*, pages 1–4.